

# Fabrication, characterization, and applications of high-performance AlGaAs-based buried-heterostructure diode lasers

Alexei V. Syrbu  
Alexandru Z. Mereutza  
Grigore I. Suruceanu  
Vladimir P. Yakovlev  
Andrei Caliman  
Anatol T. Lupu  
Stanislav Vieru

Technical University of Moldova  
168 Stefan cel Mare Avenue  
277012 Chisinau, Moldova

Marius Predescu  
Institute of Atomic Physics  
Laser Department  
P.O. Box MG-6  
76900 Bucharest-Magurele, Romania

Ion M. Popescu, MEMBER SPIE  
Radu G. Ispasoiu, MEMBER SPIE  
University Politehnica Bucharest  
Department of Physics  
Spl. Independentei 313  
77206 Bucharest, Romania

## 1 Introduction

Low-temperature (<900 K) mesa melt etching and regrowth proved to be very efficient for high-performance buried-heterostructure (BH) laser diode fabrication.<sup>1,2</sup> Low-threshold (injection current threshold  $I_{th} < 5$  mA) diode lasers (DLs) were fabricated using molecular beam epitaxy (MBE) grown strained InGaAs/AlGaAs ( $\lambda = 980$  nm) and metal-organic chemical vapor deposition (MOCVD) grown unstrained AlGaAs/GaAs ( $\lambda = 810$  nm) epitaxial structures.<sup>3,4</sup> Degradation of these DLs was determined to be caused by physicochemical processes that take place on the mirrors during operation and are enhanced by high optical power densities and increased temperatures.<sup>5</sup> Here we present data on the electro-optical and thermal properties and on the characterization of the degradation processes of these lasers. The degradation process was observed to be accelerated by single current pulses. Electro-optical and internal second-harmonic generation measurements were performed at different degradation steps. The mirror temperature values were measured by microphotoluminescence<sup>6</sup> and photothermodeflection methods.<sup>7</sup> For the InGaAs/AlGaAs structure emitting at the wavelength  $\lambda = 980$  nm and for the AlGaAs/GaAs structure emitting at  $\lambda = 810$  nm we determined excess mirror temperature values of 4 and 10 K, respectively, for operation at 60-mA injection current and 15 mW per facet. Details on the procedures for mesa shaping<sup>8</sup> are reported.

We also present the results of optical and thermal characteristic studies of 960- to 980-nm emission wavelength,

**Abstract.** Data are presented on buried-heterostructure (BH) AlGaAs/GaAs and InGaAs/AlGaAs quantum-well diode lasers (DLs) fabricated by low-temperature liquid phase mesa melt etching and regrowth. The basic laser structures were grown by either molecular beam epitaxy (MBE) or metal-organic chemical vapor deposition (MOCVD). Native oxides were used as a mask in the processes of melt etching and regrowth. Measurements of excess mirror temperature and parameters of internal second-harmonic generation (SHG) were used for DL characterization. The equalization of beam divergence in both planes, perpendicular and parallel to the active layer, was accomplished by using cylindrical microlenses, at 1 W of radiant power in continuous-wave (cw) operation. The results on medical applications and pumping Er<sup>3+</sup>-doped YAG crystals are reported. © 1996 Society of Photo-Optical Instrumentation Engineers.

Subject terms: diode laser characterization; technological and medical applications of diode lasers.

Paper RMA-07 received July 25, 1995; revised manuscript received Oct. 30, 1995; accepted for publication Nov. 17, 1995.

strained quantum well AlGaAs/InGaAs buried-heterostructure lasers with 50- and 100- $\mu$ m active layer widths, and 0.6 to 0.7-mm cavity lengths, emitting 1 W and even more optical power in cw operation. Far-field patterns of these laser diodes were modified using cylindrical microlenses. Radiant power of 15 mW was obtained in cw emission at  $\lambda = 2.94$   $\mu$ m from an Er<sup>3+</sup>:YAG crystal optically pumped by  $\approx 600$  mW of collimated 970-nm diode laser radiation.

Active layer temperatures of these lasers were measured using the method described in Ref. 9. Mirror temperatures were determined from microphotoluminescence spectral distributions<sup>6</sup> and by the photothermodeflection method.<sup>7</sup> Diode lasers operated continuously at 1 W optical power for 1000 h, showing no essential degradation.

Finally, the effect of 940- to 980-nm, 50-mW diode laser irradiation in the treatment of degenerative rheumatic diseases was studied.

## 2 Fabrication

Single spatial mode laser diodes with threshold currents as low as 3 to 5 mA at 3- $\mu$ m active layer width and 0.4- to 1.3-mm cavity length were fabricated using selective mesa melt etching and liquid phase epitaxy (LPE) regrowth.<sup>1</sup> In this work the quality of buried heterostructures was considerably improved by using AlGaAs native oxides as a mask in melt etching and regrowth liquid phase epitaxial processes.

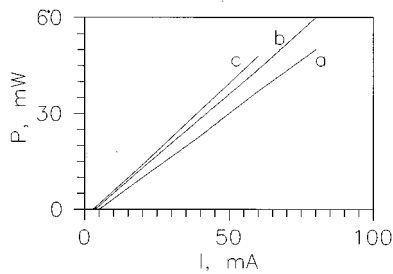


**Fig. 1** Light-current characteristics of AlGaAs/GaAs ( $\lambda=810$  nm) unstrained quantum well active region uncoated DLs for different cavity lengths: curves a, 0.8 mm; b, 0.5 mm; and c, 0.35 mm.

As reported earlier,<sup>8</sup> melt-etched mesa shapes depend on the mask adhesiveness to the epitaxial structure in under-saturated Ga-Al-As solutions at temperatures around 900 K. In addition to the fact that adhesion of traditional masking layers such as SiO<sub>2</sub> and Al<sub>2</sub>O<sub>3</sub> is much worse than that of AlGaAs native oxide, the adhesion of these oxide layers is not uniform and depends very much on the state of multilayer epitaxial structure surface, leading to nonreproducible results. Native oxide layers were grown by anodic oxidation of Al<sub>x</sub>Ga<sub>1-x</sub>As ( $x=0.5$  to 0.6) in ammonium citrate electrolyte. The growth mechanism of native oxides provides high material quality and a uniform interface with no impurities on it. This oxide is stabilized to resist harsh conditions of melt etching by postgrowth thermal treatment. It was shown that masking properties of AlGaAs-based native oxide tremendously improve by increasing AlAs composition of AlGaAs. To form such a mask, an additional AlGaAs layer with the thickness of 200 to 300 nm is grown on the surface of the multilayer structure. To obtain a necessary mask pattern, this layer is anodized through a photoresist mask. It is very important that no undercutting beneath the mask take place in the low temperature LPE mesa melt-etching and regrowth process when using AlGaAs-based native oxides. In this case, the form of the mesa is dictated only by the anisotropy of melt etching. The AlAs concentration in the AlGaAs lateral confinement layer, grown by LPE after *in situ* mesa melt etching, was adjusted to avoid the formation of higher index lateral modes in the DL waveguides.

DL mirror reflectivities were modified by depositing multilayer thin oxide films to obtain reflectivities of 5% for the output-coupling mirror and of 90% for the rear mirror.

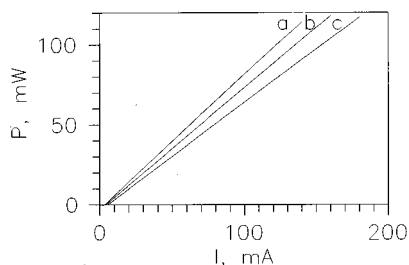


**Fig. 2** Light current characteristics of InGaAs/AlGaAs ( $\lambda=980$  nm) strained quantum well active region uncoated DLs for different cavity lengths: curves a, 0.6 mm; b, 0.9 mm; and c, 1.3 mm.

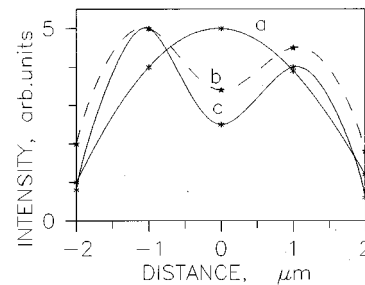


**Fig. 3** Typical near field pattern of diode lasers: the fundamental harmonic radiation before COD (curve a) and after (curve b), and second-harmonic component of the emission after COD (curve c).

Laser chips were mounted on copper heat sinks *p* side down. To reduce the beam divergence in the plane perpendicular to the active layer plane a silica cylindrical microlens with a diameter of 0.13 mm and 5 mm length was fixed with epoxy in the nearest vicinity (0.01 to 0.03 mm) of the diode laser mirror.

### 3 Characterization

Light current characteristics of InGaAs/AlGaAs and AlGaAs/GaAs BH uncoated DLs were measured in a current range that was close but did not exceed the limit of catastrophic optical degradation (COD) (Fig. 1, unstrained quantum well active region,  $\lambda=810$  nm; Fig. 2, strained quantum well active region,  $\lambda=980$  nm). The devices operate at high mirror power densities (up to 10 mW/ $\mu\text{m}^2$  of active layer width for the 810-nm DL and up to 20 mW/ $\mu\text{m}^2$  of active layer width for the 980-nm DL). A typical near-field pattern of these DLs is presented in Fig. 3, curve a. Near-field and far-field patterns were stable up to the degradation limit. Figure 4 shows the typical active layer temperatures versus driving current for InGaAs and AlGaAs lasers.

Active layer temperatures were determined using the method described by Paoli.<sup>9</sup> We attribute the better thermal behavior of 980-nm InGaAs/AlGaAs to the fact that both electrical and thermal resistance of these lasers are lower than the corresponding values for 810-nm AlGaAs/GaAs lasers. Laser mirror temperatures for 980-nm InGaAs/AlGaAs lasers were determined by the microphotoluminescence method.<sup>6</sup> The results are presented in Fig. 5. It is important to note that diode lasers that have practically the

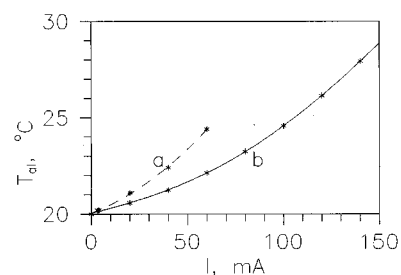


**Fig. 4** Typical active layer temperature versus driving current for InGaAs (solid line) and AlGaAs (dashed line) lasers.

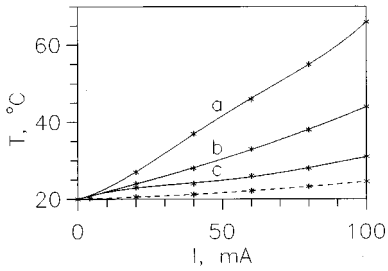


**Fig. 5** Mirror temperatures (solid lines) versus driving current for three InGaAs/AlGaAs ( $\lambda=980$  nm) diode lasers that have practically the same light-current ( $P-I$ ) and active layer temperature (dashed line)  $T_{al}$  versus current ( $T_{al}-I$ ) characteristics. Note the different mirror temperature versus current characteristics (curves a, b, and c) for laser diodes with the same cavity dimensions and bulk active layer temperature (dashed line).

same light-current ( $P-I$ ) and active layer temperature  $T_{al}$  versus current ( $T_{al}-I$ ) characteristics have different mirror temperature versus current characteristics. We presume that mirror temperatures of uncoated laser diodes are dependent on the mirror surface state densities, which are different for different laser diodes. This parameter influences neither the  $P-I$  nor the  $T_{al}-I$  characteristics.

The indirect energy bandgap of the cladding layers in 810-nm AlGaAs/GaAs lasers makes it very difficult to perform microphotoluminescence measurements on such structures. Mirror temperatures for such laser diodes were measured by the photothermodeflection technique.<sup>7</sup> The principle of this method is very simple. The deflection angle of a probe laser beam passing in the nearest vicinity of a laser mirror is proportional to the mirror temperature. The higher mirror temperature results in a larger deflection angle.

An eventual problem that could arise with this method is the right calibration. However, all our previous measurements of mirror and active layer temperatures have shown that at low current values near the threshold, these temperatures practically do not differ. This fact was used for the calibration of the photothermodeflection method. Figure 6 shows the plots of active layer temperature and photothermal deflection angle data versus driving current.

As we can see in Figs. 5 and 6, the difference between mirror temperature  $T_m$  and driving current ( $T_m-I$ ) characteristics for InGaAs/AlGaAs and AlGaAs/GaAs lasers is

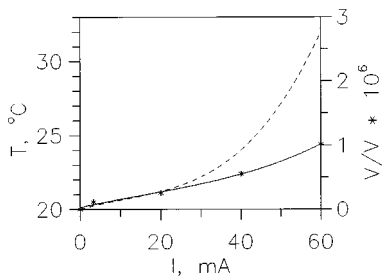


**Fig. 6** Plots of active layer temperature (solid line) and photothermal deflection angle (dashed line) data versus driving current for AlGaAs/GaAs ( $\lambda=810$  nm) unstrained quantum well active region uncoated DLs with 0.5-mm cavity length.

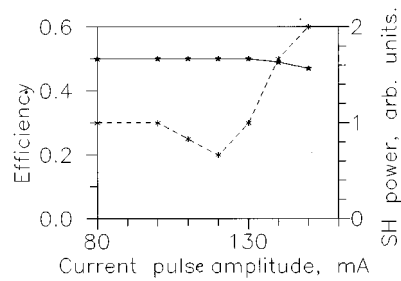


**Fig. 7** Impact of single electrical current pulses on DL efficiency and SH power for an unstrained AlGaAs active layer DL emitting at 810 nm (DL1). The FH output power of DL1 was maintained at a constant value of 10 mW/facet.

that AlGaAs/GaAs lasers have a superlinear ( $T_m-I$ ) characteristic. This superlinear dependence of mirror temperature versus driving current explains the much lower COD limit of AlGaAs/GaAs lasers, in comparison to InGaAs/AlGaAs strained quantum well DLs.

In the emission spectra of semiconductor lasers, the fundamental harmonic (FH) at the frequency  $\omega$  is accompanied by second-harmonic (SH) radiation at the frequency  $2\omega$ . The weak SH radiation, which can be observed in the output beam spectrum along with the fundamental frequency  $\omega$ , is generated in a thin near-surface layer, adjacent to the mirror facet of a laser. As we reported,<sup>10,11</sup> the intensity of SH radiation is an indicative of the DL operation regime: the larger SH intensity corresponds to increased optical power density on the mirror and greater risk of COD. The procedure of DL degradation study consisted of applying single current pulses, of different amplitudes, superimposed on a dc bias current and measuring the laser efficiency at a given constant optical output as well as near-field distribution and SH signal intensity.<sup>8</sup> For this study, we considered two typical DL configurations, here simply denoted as DL1 and DL2, for which the light-current characteristics are shown in Fig. 1, curve a, and in Fig. 2, curve b, respectively. Light-current characteristics of these diode lasers were measured in a current range that was close to but did not exceed the limit of COD. For DL1, a cw FH power of 10 mW/facet was maintained during the study. Single current pulses of 80 and 100 mA did not change the efficiency, the value of the SH signal (Fig. 7) and near-field (NF) distribution (Fig. 3, curve a). Other two current pulses of 100 and 120 mA caused a small decrease of the SH signal while the efficiency did not change. The NF distribution of the fundamental emission of this DL did not change either. The next 140-mA pulse caused a  $3\times$  decrease of efficiency, an alteration of the NF (Fig. 3, curve b), and a  $2\times$  increase of the SH power. Instead of the central lobe in the NF distribution (Fig. 3, curve a), a minimum appeared on this distribution after degradation (curve b). Note that the SH NF pattern (Fig. 3, curve c) reflects more evidently the nonuniform field distribution in laser waveguide than the FH NF pattern. The next single-current pulse with the amplitude of 150 mA caused COD.

As a result of the degradation, black spots appeared on both laser mirrors. For DL2, a cw FH power of 15 mW/facet was maintained during the study. Three single-current pulses with amplitudes from 0.1 to 0.25 A did not alter the

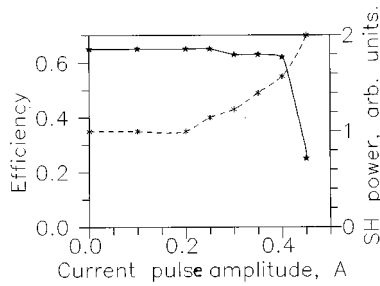


**Fig. 8** Impact of single electrical current pulses on DL efficiency and SH power for a strained InGaAs active layer DL emitting at 980 nm (DL2). The fundamental harmonic output power of DL2 was maintained at a constant value of 15 mW/facet.

values of the SH signal, DL efficiency (Fig. 8), and NF pattern. A current pulse of 0.3 A caused a small decrease of efficiency and an increase of SH power. After a 0.5-A pulse, the DL could not emit at all. Both investigated DL chips were cleaved into three parts after failure: one part from the center region of the initial chip and the other two from the side parts of the cavity with length of about 100 mm.

The central parts of both chips were operable again, while the side parts could not generate light anymore. Considerable increase of the SH signal intensity, before the COD of the laser mirrors, is caused by the appearance of the nonuniformity in the NF distribution of FH emission. As one can see in Fig. 3, the impact of single electrical pulses on an operating DL results in NF alterations. A dark spot is formed on the laser diode mirror. The area of the luminous body decreases, and at a constant emitting power, the optical power density on the mirror increases. Knowing that the SH intensity is proportional to the square of FH intensity,<sup>10</sup> the reason the SH intensity increases in the process of gradual laser diode degradation becomes clear.

In the case of the AlGaAs/InGaAs wide-strip lasers, the asymmetry of far-field pattern is quite large and this leads to difficulties when these lasers are applied for pumping solid state lasers. To overcome this problem we have used silica microlenses that were properly aligned and fixed in the vicinity of DL mirrors. Far-field pattern distributions in

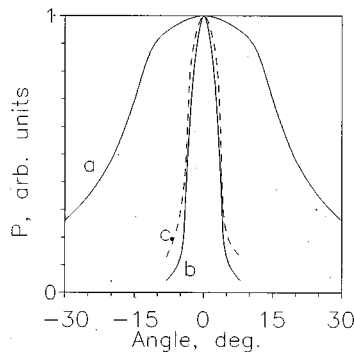


**Fig. 9** Far-field pattern distributions in the planes perpendicular (curve a) and parallel (curve c) to the active layer plane of a diode laser with 0.1-mm active layer width. Curve c shows the perpendicular distribution after fixing the microlens.

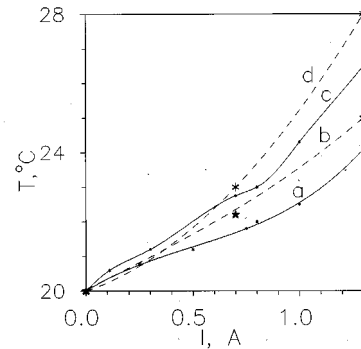


**Fig. 10** Active layer (curves a and c) and mirror (curves b and d) temperatures plotted versus DL operating current for DLs with 50  $\mu\text{m}$  (curves c and d) and 100  $\mu\text{m}$  (curves a and b) active layer widths. The heat sink temperature was maintained at 20°C.

the planes perpendicular and parallel to the active layer plane of a DL with 0.1-mm active layer width are shown in Fig. 9, curves a and b, respectively. After fixing the microlens, the far-field distribution in the parallel plane practically does not change, while the perpendicular distribution changes dramatically in curve c and is nearly the same as in curve b. Optical power measurements have shown that 80% of all optical power is concentrated in a cone with an angle of 6 deg.

Active layer temperature versus DL operating current characteristics are presented in Fig. 10. Active layer temperatures were determined using the method described in Ref. 9. After threshold, the rate of temperature increase is smaller than in the current range between 0 and threshold because a part of the electrical power applied to the diode is converted into the optical emission. By increasing the operating current, however, the heat generated in the laser active resistance becomes important and gradually increases the rate of active layer temperature rise for both DLs.

Thermal resistance values are 3 K/W for the laser of 0.05-mm active layer width and 1.6 K/W for the laser of 0.1-mm active layer width.

Excess mirror temperatures related to the temperature in the bulk of the laser diode have been determined either from the shift of microphotoluminescence spectra of the mirror facets<sup>6</sup> or from measurements of the deflection angles of a probe laser beam passing over the mirror<sup>7</sup> at different laser diode operating currents. The results are presented in Fig. 10. The shape of the dependence of the deflection angle on the operating current (curves b and d) follows the active layer temperature versus current dependence. The excess mirror temperature value determined from microphotoluminescence distribution, at 1-W emitted power, was used as a reference point for calibrating the photothermodeflection data.

Because the wide-strip DLs studied in this paper did not show any substantial degradation during 1000 h of continuous operation, we can conclude that excess mirror temperatures of the order of 10 K do not cause catastrophic optical degradation.

## 4 Applications

InGaAs/AlGaAs DLs with the emission wavelength around 970 nm and emitting on a single spatial mode have been successfully used for pumping an  $\text{Er}^{3+}$ -doped YAG crystal (with 50% concentration of  $\text{Er}^{3+}$ ) to obtain laser emission. The  $\text{Er}^{3+}$ :YAG active crystal was a 1-mm-thick slab having square flat surfaces, with 25 mm<sup>2</sup> area, perpendicular to the direction of pumping and lasing. DL mirrors were first coated with epitaxial ZnSe with the thickness of 120 nm, then with a sequence of high reflective (HR) and antireflective (AR) Si-SiO<sub>2</sub>-based layers. This procedure enabled us to increase the emitting power density on one facet up to 20 mW/ $\mu\text{m}$  of active layer width. For the DL-pumped solid state laser operation, we used the end-pumping configuration with a monolithic solid state laser resonator. For this purpose, dichroic mirrors were deposited on the end surfaces of the  $\text{Er}^{3+}$ :YAG laser crystal, for 5% reflectivity at 970 nm and 97% reflectivity at 2.94  $\mu\text{m}$  on the front (pumping) surface and 97% reflectivity at 2.94  $\mu\text{m}$  on the rear (output coupling) surface. DL emission was collimated to a 2-mm-diam beam by a cylindrical microlens, as described in Sec. 2, together with a spherical lens. The beam had  $\pm 2$  mrad divergence. For the laser power measurements, a Quantronix powermeter was used. The pump beam power threshold for  $\text{Er}^{3+}$ :YAG lasing was about 450 mW and, at a pump optical power of 600 mW, 15-mW power of radiation emitted at 2.94  $\mu\text{m}$  was measured. The energy conversion efficiency is far from optimum but our experiment demonstrated the suitability of using our DL in pumping solid state lasers. Work is in progress for improving the cavity geometry and coating procedures.

In GaAs/AlGaAs lasers, with the emission wavelength of 950 nm and optical power of 20 to 50 mW, with an operating injection current lower than 100 mA, were used to fabricate portable laser therapy apparatuses that have been successfully used in rheumatology. To find information about any positive effect of DL irradiation for the cure of such diseases, a study was carried out on patients with chronic rheumatic degenerative diseases at the N. G. Lupu Institute of Internal Medicine, Bucharest.<sup>12</sup> The patients had shown unsatisfactory response to antiinflammatory nonsteroid (AINS) therapy or presented major counterindications for AINS therapy, such as gastroduodenal ulcer. The diagnosis of these diseases was made by the usual clinical and paraclinical means. Treatment with laser radiation was administered to 136 patients grouped in pathological categories as follows: 74 patients with painful spine (46 at lumbar level, 22 at cervical level, and 6 at thoracic level), 34 with knee osteoarthritis, 8 with ankle osteoarthritis, and 20 with painful shoulder.

Every patient was treated for 10 days by daily exposures to near-IR laser radiation. In one irradiation session, one or more areas of maximum interest were submitted to the laser beam, depending on the disease. Each area was irradiated for 7 min. For all the diseases considered, the pain decreased gradually from the first to the tenth day. The greatest decrease rate of pain was observed for thoracic vertebrae osteoarthritis in which, after 7 days of treatment, the patients no longer had pain. The worst evolution was that of ankle and knee osteoarthritis.

## 5 Summary

The quality of AlGaAs-based BH lasers has been considerably improved by using an AlGaAs native oxide mask for *in situ* mesa melt etching and LPE regrowth. No undercutting process occurred using this method and the shape of the mesas is dictated only by the anisotropy of melt etching.

The uncoated BH DLs with the active layer width of 3  $\mu\text{m}$  and less can emit in a single spatial mode. The maximum optical power is 10 mW/ $\mu\text{m}$  of active layer width for AlGaAs/GaAs lasers and 20 mW/ $\mu\text{m}$  of active layer width for InGaAs/AlGaAs lasers. The higher optical power of InGaAs/AlGaAs lasers is attributed to lower electrical and thermal resistance and to linear mirror temperature versus current characteristics. Internal SH generation studies have confirmed that AlGaAs-based DLs degrade because of the mirror damage at high optical power densities and increased temperature.

BH AlGaAs-based laser diodes have been successfully used in the first approaches of pumping  $\text{Er}^{3+}$ :YAG lasers and in the treatment of chronic rheumatic degenerative diseases.

### Acknowledgment

This work was supported in part by the International Scientific Foundation, grant MY-4000.

### References

1. Z. I. Alferov, V. M. Andreyev, A. V. Syrbu, A. Z. Mereutza, and V. P. Yakovlev, "Extremely low threshold AlGaAs buried heterostructure quantum well laser diodes grown by LPE," *Appl. Phys. Lett.* **57**, 2873–2875 (1990).
2. N. Chand, S. N. G. Chu, N. K. Dutta, J. Lopata, M. Geva, A. V. Syrbu, A. Z. Mereutza, and V. P. Yakovlev, "Growth and fabrication of high performance 980-nm strained InGaAs quantum well lasers for erbium doped fiber amplifiers," *IEEE J. Quantum Electron.* **30**(2), 424–440 (1994).
3. A. V. Syrbu, A. Z. Mereutza, V. P. Yakovlev, G. I. Suruceanu, and A. T. Lupu, "Buried heterostructure AlGaAs photonic devices fabricated by low temperature mesa melt-etching and regrowth," *J. Electron. Mater.* **5**, 710–714 (1994).
4. V. P. Yakovlev, A. T. Lupu, A. V. Syrbu, A. Z. Mereutza, I. V. Kravetsky, and L. L. Kulyuk, "Characterization of the degradation processes in the buried heterostructure quantum well lasers using internal second harmonic emission," presented at MRS Fall Meeting, Boston, November 28–December 2, 1994.
5. H. Brugger and P. W. Epperlein, "Study of correlation between degradation and local mirror facet temperature of the active region in high-power SQW InGaAs/GaAs, AlGaAs/GaAs and InGaAsP/GaAs laser diodes under cw operation," *Appl. Phys. Lett.* **56**, 1049–1051 (1990).
6. P. W. Epperlein, P. Buchmann, and A. Jakubowicz, "Lattice disorder, facet heating and catastrophic optical mirror damage of AlGaAs quantum well lasers," *Appl. Phys. Lett.* **62**(5), 455–457 (1993).
7. M. Bertolotti, G. Liakhov, R. Li Voti, R. P. Wang, C. Sibilina, V. P. Yakovlev, "Mirror temperature of a semiconductor diode laser studied with a photothermal deflection method," *J. Appl. Phys.* **74**, 7054–7060 (1993).
8. A. Z. Mereutza, A. V. Syrbu, and V. P. Yakovlev, "Buried heterostructure formation processes for high performance devices," in *Proc. 15th Ann. Semiconductor Conf.*, pp. 455–458, Romanian Academy, Sinaia, Romania (Oct. 1992).
9. T. L. Paoli, "A new technique for measuring the thermal impedance of junction lasers," *IEEE J. Quantum Electron.* **QE-11**, 498–503 (1975).
10. I. V. Kravetsky, L. L. Kulyuk, A. T. Lupu, D. A. Shutov, G. I. Suruceanu, A. V. Syrbu, and V. P. Yakovlev, "Internal second harmonic generation in CW AlGaAs SQW lasers: the facet degradation monitoring," *Appl. Surface Sci.* **69**, 424–428 (1993).
11. V. P. Yakovlev, A. T. Lupu, A. V. Syrbu, G. I. Suruceanu, I. V. Kravetsky, L. L. Kulyuk, and N. Chand, "Characterization of strained quantum well InGaAs/AlGaAs buried heterostructure lasers using internal second-harmonic generation," presented at Laser Diode Tech-

nology and Applications VI, SPIE Tech. Conf. 2148C, Los Angeles (1994).

12. C. Fulga, I. G. Fulga, and M. Predescu, "Clinical study of the effect of laser therapy in rheumatic degenerative diseases," *Rom. J. Intern. Med.* **32**(3), 227–233 (1994).

**Alexei V. Sybru** received a degree in electronic engineering in 1972 from the Technical University of Moldova and a PhD in 1979 from the Institute of Applied Physics, Moldova Academy of Sciences. Since 1972 he has been with the Laboratory of Optoelectronics of the Technical University of Moldova. In 1976 and 1977 he conducted research at A. F. Ioffe Institute, Sankt-Petersburg. In 1982 and 1990 he was a visiting fellow at Sheffield University, UK. His research has concerned AlGaAs/GaAs and InGaAsP/InP liquid phase epitaxy growth and melt-etching selectivity, new processes for high-performance light-emitting device fabrication, and diode laser characterization. In 1983, Dr. A. Sybru was awarded the Soviet Union prize for contribution to light-emitting devices.

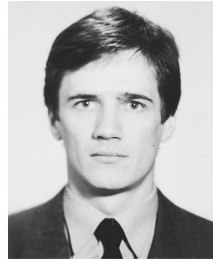
**Alexandru Z. Mereutza** received a degree in physics in 1983 from the Chisinau State University. Since 1986 he has been with the Laboratory of Optoelectronics of the Technical University of Moldova. His research interests include the III-IV epitaxial growth of diode laser structures.



**Grigore I. Suruceanu** received a degree in physics from the Chisinau State University in 1983. Since 1986 he has been with the Laboratory of Optoelectronics of the Technical University of Moldova. His research interests include semiconductor lasers and new optoelectronic devices on III-IV epitaxial structures.



**Vladimir P. Yakovlev** received a degree in electronic engineering in 1973 from the Technical University of Moldova and a PhD in 1985 from the Institute of Applied Physics, Moldova Academy of Sciences. His dissertation dealt with the fabrication, characterization, and analysis of AlGaAs/GaAs injection lasers with lateral mode control using liquid phase epitaxy and *in situ* melt back, under the guidance of Prof. J. Alferov. Since 1973 he has been with the Laboratory of Optoelectronics of the Technical University of Moldova, where his work has involved the growth and fabrication of solar cells and semiconductor lasers and their application in fiber optics, medicine, etc. His current research interests include epitaxial growth, semiconductor lasers, and optical communications.



**Andrei Caliman** received a degree in physics from the Chisinau State University in 1983. Since 1986 he has been with the Laboratory of Optoelectronics of the Technical University of Moldova. His research interests include semiconductor lasers and new optoelectronic devices on III-IV epitaxial structures.

**Anatol T. Lupu** received a degree in physics from the Moscow Physics Engineering Institute in 1985. Since 1986 he has been with the Laboratory of Optoelectronics of the Technical University of Moldova. His research interests include diode lasers and nonlinear optical interactions.

**Stanislav Vieru** received a degree in physics from the Chisinau State University in 1986. Since 1986 he has been with the Laboratory of Optoelectronics of the Technical University of Moldova. His research interests include semiconductor lasers and new optoelectronic devices on III-IV epitaxial structures.



**Marius Predescu** graduated from the Faculty of Electrical and Computer Engineering, University Politehnica Bucharest, in 1978. Presently he is with the Laser Department of the Institute of Atomic Physics, Bucharest-Magurele. His main research interests are diode laser optical pumping of solid state lasers and applications of diode lasers in medicine.

**Ion M. Popescu:** Biography and photograph appear with the special section guest editorial in this issue.



**Radu G. Ispasoiu** received the MSc degree in physics from the Faculty of Physics, Bucharest University, in 1991. In the academic year 1992/1993 he was a visiting graduate student at Clarendon Laboratory, University of Oxford, UK, where he conducted research on optical properties of GaAs/AlGaAs quantum-well structures. Presently, he is with the Department of Physics, University Politehnica Bucharest. His research interests are optical and charge transport properties of semiconductor nanostructures and their optoelectronic applications.